Structure *14*, 1083–1092, June 2006 DOI 10.1016/j.str.2006.05.010

Structure of Artemin Complexed with Its Receptor GFRα3: Convergent Recognition of Glial Cell Line-Derived Neurotrophic Factors

Xinquan Wang,[1] Robert H. Baloh,[2] Jeffrey Milbrandt,[3] and K. Christopher Garcia[1,*]
[1] Howard Hughes Medical Institute
Stanford University School of Medicine
Departments of Microbiology and Immunology, and Structural Biology
Stanford, California, 94305-5124
[2] Department of Neurobiology
Washington University School of Medicine
St. Louis, Missouri 63110
[3] HOPE Center for Neurological Disorders
Departments of Pathology and Neurology
Washington University School of Medicine
St. Louis, Missouri 63110

Summary

Artemin (ARTN) is a member of the glial cell line-derived neurotrophic factor (GDNF) family ligands (GFLs) which regulate the development and maintenance of many neuronal populations in the mammalian nervous system. Here we report the 1.92 Å crystal structure of the complex formed between ARTN and its receptor GFRα3, which is the initiating step in the formation of a ternary signaling complex containing the shared RET receptor. It represents a new receptor-ligand interaction mode for the TGF-β superfamily that reveals both conserved and specificity-determining anchor points for all GFL−GFRα pairs. In tandem with the complex structure, cellular studies using receptor chimeras implicate dyad-symmetric composite interfaces for recruitment and dimerization of RET, leading to intracellular signaling. These studies should facilitate the functional dissection of the specific versus pleiotropic roles of this system in neurobiology, as well as its exploitation for therapeutic applications.

Introduction

The glial cell line-derived neurotrophic factor (GDNF) family ligands (GFLs) include GDNF (Lin et al., 1993), neurturin (NRTN) (Kotzbauer et al., 1996), persephin (PSPN) (Milbrandt et al., 1998), and artemin (ARTN) (Baloh et al., 1998). GFLs play critical roles in supporting the development and survival of distinct sets of central and peripheral neurons (Airaksinen and Saarma, 2002; Baloh et al., 2000a). The potent neurotrophic activities of GFLs have stimulated interest in their use as therapeutic agents for the treatment of neurodegenerative diseases such as Parkinson's. GDNF, the founding member in the family, has shown antiparkinsonian actions in various animal models and pilot studies with human patients (Gill et al., 2003; Grondin and Gash, 1998; Slevin et al., 2005). ARTN has been shown in recent studies to be effective as a systemic treatment for neuropathic pain (Gardell et al., 2003). Given the importance of GFLs in basic neurobiology and their potential therapeutic value, it has become a compelling goal to understand the molecular basis of the interactions between GFLs and their receptors.

GFLs belong to the transforming growth factor β (TGF-β) family because of the conserved seven cysteine residues and structural similarities, but they are different from other members in the signaling pathway (Saarma, 2000). Unlike other members in the TGF-β family (TGF-βs, BMPs, Activins, etc.) which signal through direct engagement of two different types of serine/threonine receptor kinases (Massague and Chen, 2000), GFLs exert their activities through the nucleation of a ternary complex containing a nonsignaling, ligand-specific GFRα receptor and a signaling and shared tyrosine kinase receptor RET (Durbec et al., 1996; Treanor et al., 1996; Trupp et al., 1996; Worby et al., 1996). One widely accepted model is that GFL first binds its preferential GFRα receptor. This binary complex, then, recruits RET through the formation of a composite GFL/GFRα interface, which triggers the activation of the intracellular tyrosine kinase domain (Airaksinen et al., 1999). The GFRα receptors contain three cysteine-rich repeats that appear to mark distinct extracellular domains (D1, D2, and D3). Four different GFRα receptors (GFRα1-4) have been identified (Baloh et al., 1998; Buj-Bello et al., 1997; Enokido et al., 1998; Jing et al., 1996), and it is now established that GFRα1 binds preferentially to GDNF, GFRα2 to NRTN, GFRα3 to ARTN, and GFRα4 to PSPN (Airaksinen et al., 1999).

The protein fold of GDNF is a canonical "cystine-knot" motif, formed by a hallmark pattern of seven cysteine residues within the primary sequence, and one interchain disulfide bond linking two GDNF monomers to form a homodimer (Eigenbrot and Gerber, 1997; Sun and Davies, 1995). The structure of a single unliganded domain corresponding to the third cysteine-rich repeat (D3) of GFRα1 has been reported, which did not posses ligand binding activity, but from which the GDNF interactions were modeled (Leppanen et al., 2004). In order to begin to elucidate the molecular basis of GFL receptor recognition and activation, we report here the crystal structure of ARTN bound to the ligand binding domains of GFRα3, together with cellular studies that collectively point to a convergent binding and activation mode between GFL and their receptors across this important neurotrophic factor family.

Results

Biochemical Studies and Structure Determination

A soluble ectodomain of human GFRα3 (D1D2D3) (residues 32–363) with a C-terminal hexa-histidine tag, and human ARTN (residues 139–237) without His-tag were coexpressed in insect cells. Gel filtration chromatography of the Nickel-agarose captured material resolved a major peak consisting of the ARTN−GFRα3 complex, followed by excess GFRα3 (Figure 1A). The molecular weight of the ARTN−GFRα3 complex determined by

*Correspondence: kcgarcia@stanford.edu

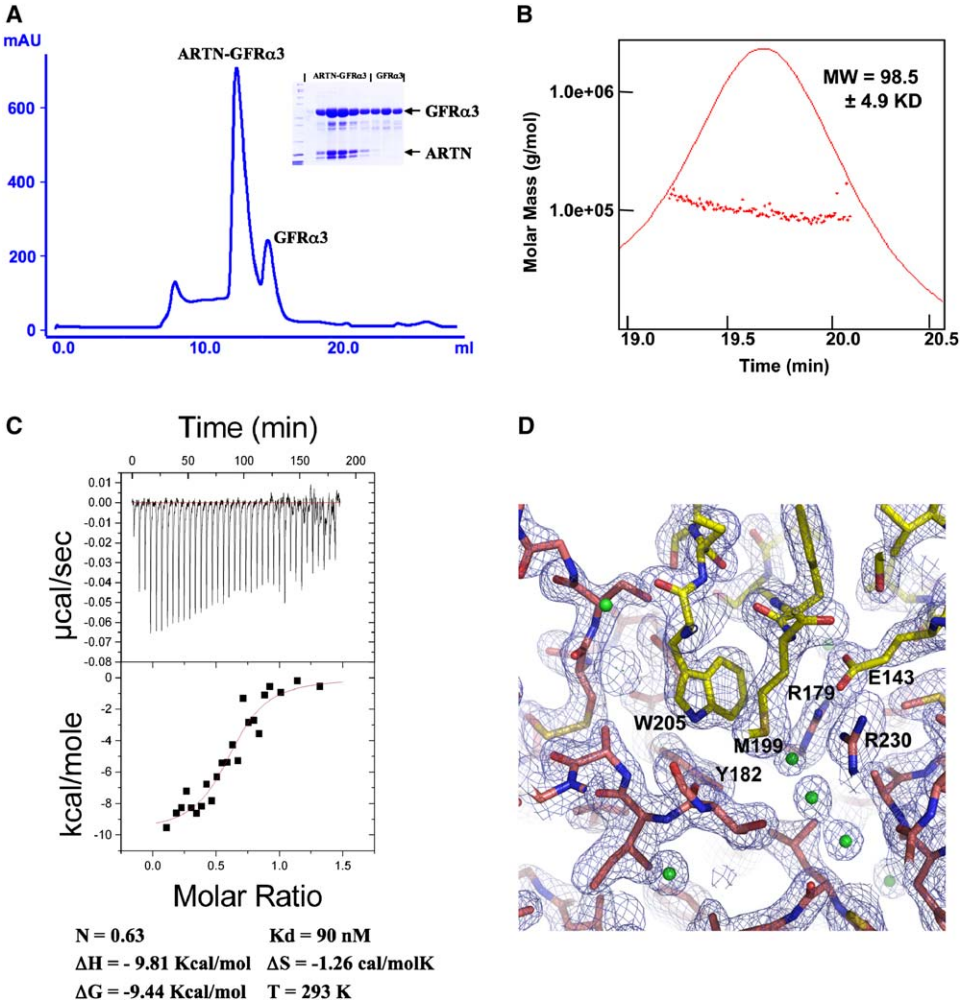

Figure 1. Biochemical and Structural Characterization of the ARTN−GFRα3 Complex

(A) Gel filtration analysis of the ARTN−GFRα3 (D1D2D3) complex. ARTN without hexa-histidine tag copurifies with GFRα3 molecules containing hexa-histidine tag.

(B) Measurement of the molecular weight of the ARTN−GFRα3 (D1D2D3) complex by multiangle laser light scattering (MALS). The measured 98.5 kDa molecular weight is consistent with the 1:2 stoichiometry in the ARTN−GFRα3 complex (calculated MW = 97.2 kDa).

(C) Isothermal titration calorimetry (ITC) of GFRα3 receptor with ARTN. The N value of 0.63 indicates a 1:2 stoichiometry of one ARTN dimer binding to two GFRα3 monomers. The theoretically correct value of N = 0.5 is in practice difficult to obtain due to the slight imprecision in protein concentration measurements using different methods. The affinity value of K_d = 90 nM compares to the affinity of ARTN for GFRα3 measured on cells giving a K_d = 1-10 nM. The lower affinity is what is commonly observed when receptor affinities are measured with soluble molecules in a free solution state compared to the receptors being constrained to the cell surface. In the solution state, there is a rigid body entropy penalty (rotation and translation) that results in a reduction in the observed binding free energy.

(D) A representative electron density map (SIGMAA 2Fo-Fc, 1.2σ) around residues Trp 205 and Met 199 in the ARTN/GFRα3 binding interface. Several water molecules mediate hydrogen bonds at the perimeter of the interface, but there are no buried waters within the tightly packed core.

multiangle laser light scattering (MALS) is 98.5 kDa (Figure 1B), indicating the complex consists of two receptor molecules and one ARTN homodimer. The 1:2 stoichiometry was further validated by isothermal titration calorimetry (Figure 1C), which indicated that the complex is composed of one ARTN homodimer and two GFRα3 (D1D2D3) receptors.

During crystallization, the GFRα3 N-terminal domain (D1) was spontaneously proteolyzed by remaining trace quantities of proteases after purification. This digestion resulted in the formation of crystals containing a complex consisting of the GFRα3 D2D3 domains (residues 146–363) and one ARTN homodimer, which was confirmed by N-terminal sequencing of washed crystals. That D1 is dispensable for ARTN−GFRα3 complex formation is consistent with previous findings that GFRα4 as well as some isoforms of GFRα2 do not contain a D1, indicating it is not required for GFL binding or recruitment of RET (Airaksinen et al., 1999; Scott and Ibanez, 2001). A combination of heavy atom phasing and molecular replacement methods were used to determine the complex structure at 1.92 Å resolution, as well as two different unbound ARTN structures at resolutions of 1.76 Å and 2.6 Å, respectively (Figure 1D and Table 1).

Overall Structure of the ARTN-GFRα3 Complex

The complex consists of a single ARTN homodimer together with two GFRα3 D2D3 molecules in a 1:2

Table 1. Crystallographic Statistics

	GFRα3-ARTN complex	ARTN (form 1)	ARTN (form 2)	ARTN derivative (Hg)
Data collection[a]				
Space group	$P2_1$	$P6_522$	$P6_5$	$P6_5$
Cell dimensions				
a, b, c (Å)	73.7, 41.5, 119.9	47.9, 47.9, 190.1	94.2, 94.2, 219.2	94.4, 94.4, 219.5
α, β, γ (°)	90, 103.6, 90	90, 90, 120	90, 90, 120	90, 90, 120
Resolution (Å)	40.0-1.92	40.0-1.76	40.0-2.60	40.0-2.80
R_{merge}	8.1 (51.5)	7.4 (54.8)	8.8 (59.4)	6.6 (33.3)
I / σI	21.0 (3.0)	42.5 (2.4)	24.2 (2.9)	20.7 (3.0)
Completeness (%)	98.9 (98.5)	89.4 (96.4)	99.8 (100)	99.3 (97.1)
Redundancy	11.8	21.2	18.0	9.2
Refinement				
Resolution (Å)	50.0-1.92	50-1.76	50-2.6	
No. reflections	54357	13670	33810	
R_{work} / R_{free}	21.9/26.6	23.9/25.5	30.8/35.3	
No. atoms				
Protein	4574	736	4416	
Water	236	113		
Carbohydrate	61			
B-factors				
Protein	37.3	38.1	43.9	
Water	39.2	41.3		
Carbohydrate	42.4			
Rms deviations				
Bond lengths (Å)	0.021	0.016	0.04	
Bond angles (°)	1.82	1.78	3.24	

[a] Number in the parentheses are statistics for the highest resolution shell.

stoichiometry (Figures 2A and 2B). One symmetric ARTN dimer binds two GFRα3 molecules at each of its two distal tips, resulting in the complex spanning ~130 Å in the dimension parallel to the cell membrane (Figure 2A). The noncrystallographic 2-fold related halves of the complex are highly similar to each other (Figure 2B), being related by a rotation of ~179° and with a root-mean-square difference (rmsd) of ~0.6 Å for 298 Cα positions.

ARTN Homodimer

ARTN is a homodimer in which the two monomers are assembled in a "tail-to-head" fashion, linked by an interchain disulfide bond (Figures 2A and 2B). The ARTN monomer structure is composed of two β sheet fingers, a cystine-knot core motif, and an α-helical heel region. The finger 1 is composed of two long continuous antiparallel β strands, and finger 2 has interruptions in the middle, resulting in five relatively short β strands in the β sheet. In the dimer, the helix in the heel region of one ARTN monomer contacts the finger region of another monomer with its helical axis nearly perpendicular to the β strands (Figures 2A and 2B). The structure of ARTN bound to GFRα3 is very similar to the two unbound structures, as reflected in the rmsd of ~1 Å for Cα superimposition in both monomer and dimer levels. Structural comparison of ARTN with GDNF shows an approximate 20° difference in the angle between the finger and heel regions, which results in poor monomer superimposition (~7 Å rmsd) and different homodimer orientations (Figures S1B and S1C; see the Supplemental Data available with this article online).

GFRα3 "D2D3" Module

The compact globular structure of the GFRα3 D2D3 fragment was unexpected based on speculation that the GFRα fold into three independent domains (Leppanen et al., 2004). Instead, the "D2D3" modules are closely packed together, with each cysteine-rich repeat domain contributing five α helices (α1–α5 for D2, α6–α10 for D3) that then stack in two roughly triangular spirals (Figure 2C). The interface between the two domains forms a large hydrophobic core between the outermost helices (α3 and α4) of the D2 domain with the innermost helices (α8, α10 and α8-α9 linker) of the D3 domain, respectively. The residues involved in the hydrophobic interactions include Leu200, Phe204, Leu216, Leu217, Leu289, Tyr292, Leu293, Ile296, Phe304, and Ile345, which are highly conserved in all GFRα receptors. The disulfide-bond pattern is very similar in both D2 and D3, which has five disulfide bonds distributed at the three corners of the triangular spiral to fix the scaffold (Figure 2C). There are no disulfide bonds in the interface between D2 and D3. Considering that all cysteine residues in the disulfide-bonds are conserved across the GFRα family and the correspondence of GFRα3 D3 to the isolated GFRα1 D3 domain previously solved (rmsd of ~0.6 Å for 62 Cα atoms in the helical region) (Leppanen et al., 2004) (Figure S1A; see the Supplemental Data available with this article online), we believe that other GFRα receptors will have similar architectures.

Overview of the ARTN/GFRα3 Binding Interface

The interaction of ARTN with GFRα3 occurs through the protruding tips of fingers 1 and 2 in ARTN inserting into a pocket in the center of a triangle of α helices in the D2 domain of GFRα3 (Figure 3A). The D3 domain has no

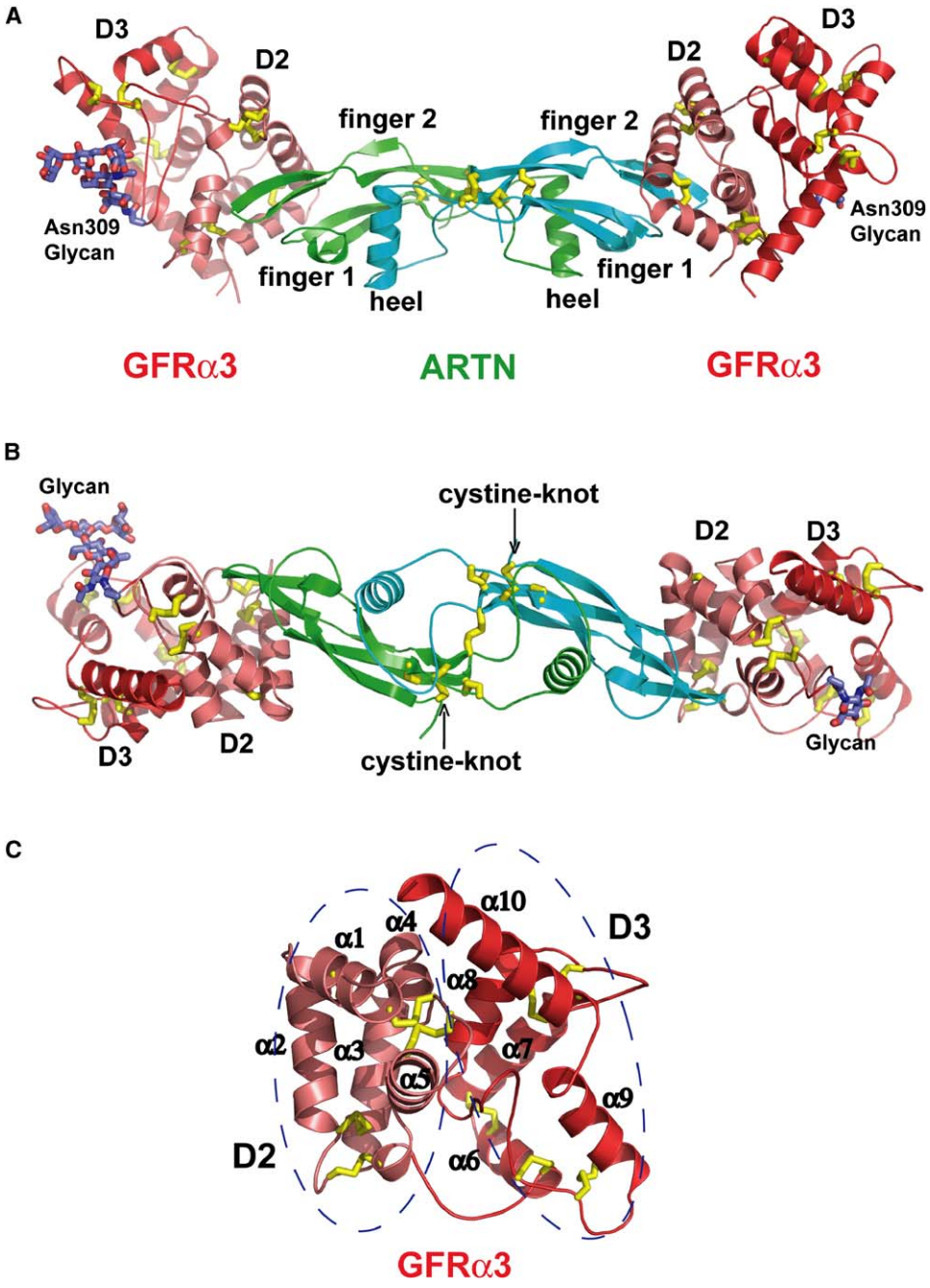

Figure 2. Overall Structure of Artemin Complexed with GFRα3

In (A), the view is approximately parallel to where a cell membrane would lie underneath the complex, in (B) the view is from above, looking down on the complex with membrane underneath (approximately a 90° rotation of the complex in (A) toward the reader. One ARTN dimer (monomers in cyan and green) binds two GFRα3 receptors. The observed N-linked carbohydrates at Asn309 position of GFRα3 are shown as sticks in dark blue.

(C) The stacked D2 and D3 subdomains in the GFRα3 receptor "D2D3" module. The D2 is shown in deep salmon color, while the D3 is shown in red. Disulfide bonds are shown in yellow. The program PyMol (DeLano, 2002) was used to make all the following figures.

interaction with ARTN. The role of the D3 domain appears to be to stabilize the D2 domain, in contrast to speculation that it forms direct ligand contacts (Leppanen et al., 2004). As a result of complex formation, 16 residues from ARTN and 19 residues from GFRα3 bury a total of ~1500 Å^2 surface (Figures 3C and 3D; also see Table S1 in the Supplemental Data available with this article online). The interface between ARTN and GFRα3 can be described as a small hydrophobic core surrounded by a much larger halo of charged and hydrophilic interactions (Figures 3C and 3D), consistent with our thermodynamic measurements indicating that binding is enthalpy driven, which is usually a signature for polar and charged interactions (Figure 1C) (Carneiro

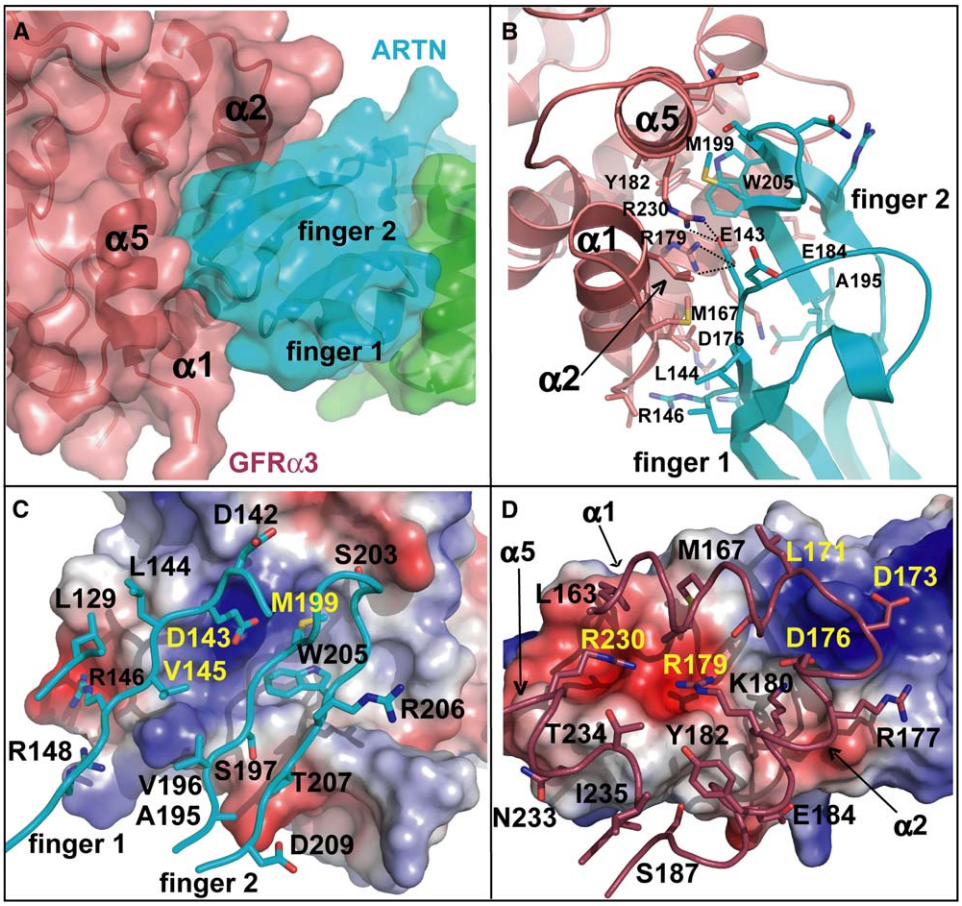

Figure 3. Ligand-Receptor Contacts between Artemin and GFRα3

(A) Molecular surfaces highlight the knob-in-hole complementarity between the protruding ARTN finger region (cyan) and the recessed center of a triangular spiral of α helices in GFRα3 D2 (deep salmon) formed by helices α1, α2, and α5.

(B) Interatomic contacts between ARTN and GFRα3, with the hydrophobic core of ARTN surrounded by a halo of polar interactions.

(C) Electrostatic footprints and complementarity of buried residues of ARTN on top of the GFRα3 surface.

(D) Electrostatic footprints and complementarity of buried residues of GFRα3 on top of the ARTN surface.

et al., 2002; He et al., 2001). Both apolar and polar segments in ARTN/GFRα3 contact interface contain conserved residues in GFLs and GFRα receptors. These conserved residues clearly serve as the common anchor points in all GFL–GFRα pairs, which are then surrounded by specificity determinants unique to each GFL–GFRα pair.

Conserved Hydrophobic and Hydrophilic Interactions

The protruding hydrophobic core at the ARTN fingertips, composed of Trp205 and Met199 (Figure 3B), is highly conserved in other GFLs (Figures 4A and 4B). It is structurally and chemically matched on the complementary GFRα3 surface formed by a recessed ring of exposing residues including Arg179, Tyr182, Gly183, Arg230, and Ala236 (Figure 4B). The main contact hydrophobic residue Tyr182 in GFRα3 is strictly conserved, and hydrophobic positions Gly183 and Ala236 are also replaced by hydrophobic residues in other GFRα receptors (Figure 4C). Upon complex formation, Trp205 and Met199 from ARTN undergo large sidechain movements and bury ~28% of the total surface area in the interface (Figure 3C; also see Figure S1D in the Supplemental Data available with this article online). Underscoring the importance of Trp205 and Met199 positions, their mutations in GDNF result in a complete loss of binding activity for GFRα1 (Eketjall et al., 1999).

The majority of the ARTN/GFRα3 interface is formed by several patches of matching complementary charge (Figures 3C and 3D). The conserved hydrophilic patch involves salt bridges between residue Glu143 from ARTN and residues Arg179 and Arg230 in GFRα3 (Figure 3B), which are strictly conserved in all GFRα receptors (Figure 4C). Glu143 is also strictly conserved in all GFLs (Figure 4A) and is one of the most important binding determinants for the interactions between GDNF and GFRα1 (Eketjall et al., 1999). We therefore speculate that these two binding epitopes, one hydrophobic and one charged, constitute "anchor" points for GFLs interactions with their GFRα receptors.

GFL-GFRα Specificity Determinants

We also find three epitopes in the ARTN-GFRα3 complex that are potential determinants of specificity between GFLs and their preferential GFRα receptors. The

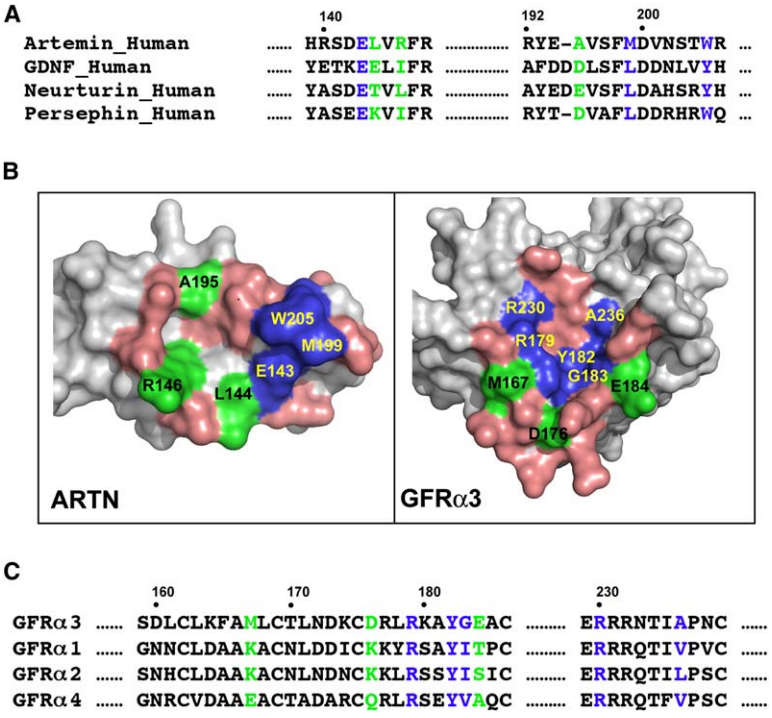

Figure 4. Conservation of Shared and Specific Ligand-Receptor Anchor Points across the GDNF Family Ligands and Receptors

(A) Sequence alignment of GFL around the region of receptor contact. The more conserved positions are colored in blue, while the more variable ligand-specific residues are colored in green to correspond with the coloring of the "open-book" surface representation, shown in panel (B) of the ARTN/GFRα3 interface.

(B) Common binding residues are colored in blue, and ligand-receptor specific residues are colored green on a background of the total buried surface (gray). ARTN is in the left panel and GFRα3 in the right panel.

(C) Sequence alignment of GDNF α receptors (GFRα) around the region of ligand contact. As for (A), the conserved positions are colored in blue, while the variable ligand-specific residues are colored in green.

first is a van der Waals interaction between positions Ala195 (ARTN) and Glu184 (GFRα3) (Figure 3B). The other three GFLs, GDNF, NRTN, and PSPN, have negatively charged residues (Asp or Glu) at position 195 (Figure 4A), and we expect that the repulsion from Asp-Glu or Glu-Glu would not favor the binding of GDNF, NRTN, and PSPN with GFRα3. Their preferential receptors GFRα1, GFRα2, and GFRα4 have small neutral residues at position 184 instead of a negatively charged residue (Figure 4C). A patch of complementary charge between Arg146 of ARTN and Asp176 of GFRα3 is another potential specificity determinant (Figure 3B). Receptors GFRα1 and GFRα2 both have Lys instead of Asp at position 176 (Figure 4C), which would result in repulsion by an Arg-Lys interaction in a mismatched ligand-receptor pair. The last potential determinant is a hydrophobic contact between Leu144 of ARTN and Met167 in GFRα3 (Figure 3B). The corresponding residues found at position 144 in GDNF, NRTN, and PSPN are Glu, Thr, and Lys, respectively, that match with Lys, Lys, and Glu, respectively, at position 167 in GFRα1, GFRα2, and GFRα4 (Figures 4A and 4C). These charge reversals would then be repulsive in mismatched complexes (GDNF-GFRa4, PSPN-GFRa1, and PSPN-GFRa2).

To probe the importance of the D2D3 region of GFRα3 for interaction with artemin as well as RET, we generated mutant chimeric receptors between GFRα2 and GFRα3 and directly test their ability to form functional ternary receptor signaling complexes in response to NRTN and ARTN, respectively (Figure 5). The experiment was done by transiently transfecting the chimeric receptor together with Gal4-Elk1/Gal4-luciferase reporter system into fibroblasts that stably express RET. This system,

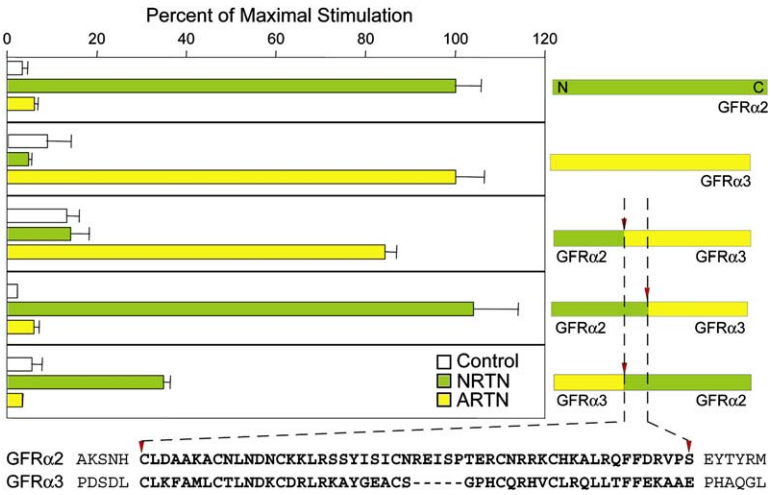

Figure 5. Functional Demonstration that Receptor Specificity for GFL Is Dictated by the D2 Domain

Substitution of GFRα3 D2 domain with that of GFRα2 results in conversion to NRTN specificity, while substitution of GFRα2 D2 domain with that of GFRα3 results in conversion to ARTN specificity. NIH-3T3 fibroblasts stably expressing human RET were transfected with the indicated construct, together with the Gal4-Elk1 fusion and a Gal4-luciferase reporter. Cells were deprived of serum, and stimulated with 50 ng/mL of the indicated ligand for 6 hr. Experiments were done in triplicate, and normalized to the response to the preferred ligand (ARTN for GFRα3, and NRTN for GFRα2). The residues in bold below correspond to the region conferring ligand specificity.

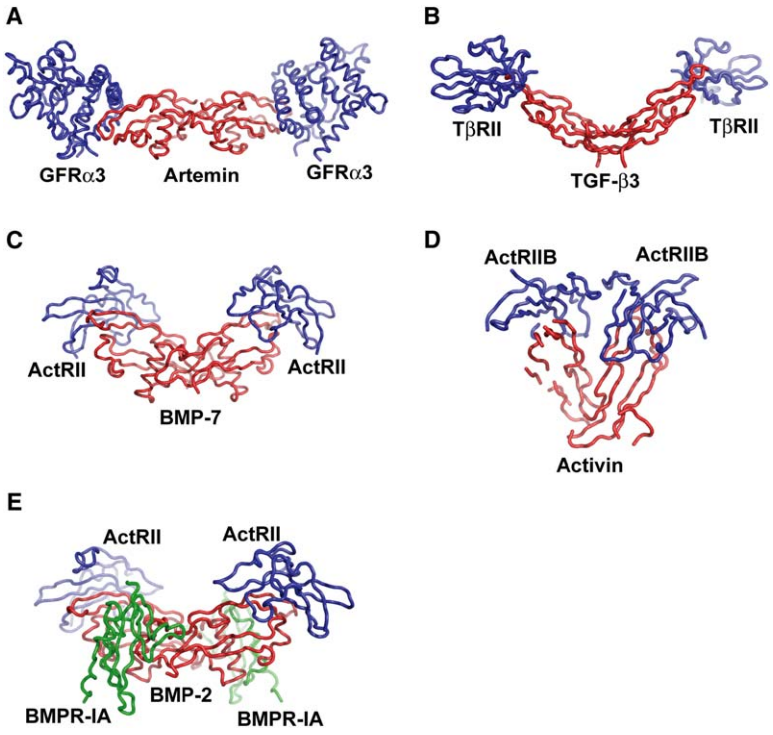

Figure 6. Diversity of Receptor-Ligand Docking Modes in the TGF-β Superfamily

Each of the complexes are shown in approximately similar orientations with respect to the ligand, and the cell membrane would lie underneath the complexes. (A) Artemin bound to GFRα3; (B) TGF-β3 bound to TβRII; (C) BMP-7 bound to ActRII ; (D) Activin bound to ActRIIB; (E) BMP-2 bound to ActRII and BMPR-1A.

which utilizes the ability of the Gal4-Elk1 fusion protein to respond to MAP kinase activity and activate transcription of the Gal4-luciferase reporter, has been used previously to monitor NGF-TrkA activation of MAP kinase in PC12 cells and GDNF-RET activation of MAP kinase in neuroblastoma cell lines (Worby et al., 1996; York et al., 1998). As expected, wild-type GFRα2 responded only to NRTN, and GFRα3 only to ARTN. A chimeric GFRα containing N-terminal GFRα2 (Ser22 to His160) together with C-terminal GFRα3 (Cys162 to Asn374) responded only to ARTN. In contrast, a chimera containing N-terminal GFRα2 (Ser22 to Ser213) with C-terminal GFRα3 (Pro210 to Asn374) responded only to NRTN, indicating that residues involved in ligand specificity lie between Cys162 and Glu209, in the D2 region of GFRα3. Confirming this, an additional chimera with N-terminal GFRα3 (Gly31 to Pro157) fused with C-terminal GFRα2 (Glu214 to Gln374), in which the D2 region was derived from GFRα2, maintained responsiveness only to NRTN. Therefore, these functional receptor studies indicate that the ligand specificity is dictated by the stretch of residues from Cys162 to Glu209, which is the major region of GFRα3 contacting ARTN in our structure.

Discussion

The activated receptor complexes of GFLs consist of the shared signaling tyrosine kinase receptor RET and ligand-specific nonsignaling GFRα coreceptors (Airaksinen and Saarma, 2002). This receptor composition is unique in the TGF-β superfamily, because other members, such as BMPs, Activins, and TGF-βs, have two different types of serine/theronine receptor kinases (Massague and Chen, 2000). Previous studies have revealed the complex structures of BMPs, Activins, and TGF-βs with their receptors, which all have one single β sheet fold in the receptor ectodomain (Figures 6B–6E) (Allendorph et al., 2006; Greenwald et al., 2003; Greenwald et al., 2004; Hart et al., 2002; Kirsch et al., 2000; Thompson et al., 2003). Our ARTN−GFRα3 complex structure adds a new ligand-receptor binding mode in the TGF-β superfamily because the GFRα3 ectodomain has multiple domains mainly composed of α helices. Although still substantially different, the overall docking mode of ARTN with GFRα3 is most similar to that seen in the TGF-β3−TβRII complex (Figures 6A and 6B) (Hart et al., 2002), which also uses the ligand fingertips to engage receptor. Structural comparison of the ligand-receptor complexes in the TGF-β superfamily also shows different intermonomer angles in the homodimeric ligands (Figures 6A–6E). Such homodimeric structural flexibility has been proposed to be a potential mechanism of receptor signaling modulation (Greenwald et al., 2004; Thompson et al., 2003). Variable homodimer orientations have also been observed between ARTN and GDNF (Figure S1C; see the Supplemental Data available with this article online), and we propose that it would result in different relative orientations of two RET molecules in the ternary signaling complex, potentially influencing the activation of its intracellular kinase domains.

GFL must engage GFRα in order to recruit the shared tyrosine kinase receptor RET (Airaksinen and Saarma, 2002), suggesting that RET recognizes a composite surface formed by the conjunction of GFL and GFRα receptor (Scott and Ibanez, 2001; Trupp et al., 1998). Alternatively, ligand capture by GFRα on the membrane may increase the effective concentration of GFL at the cell surface for presentation to RET through a noncomposite RET binding surface on GFL, or the GFL binding will induce the conformational changes of the noncomposite

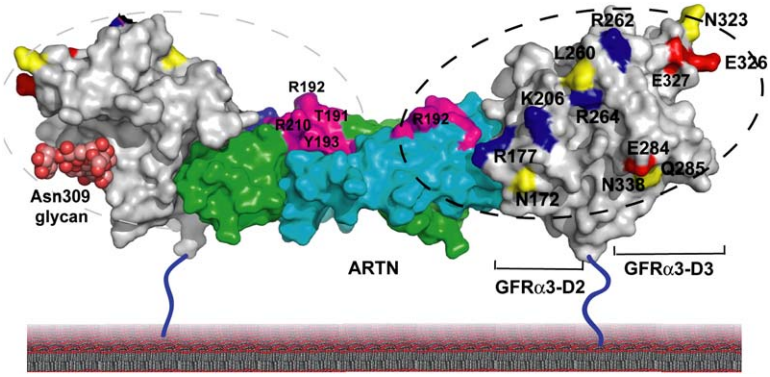

Figure 7. Putative RET Binding Surface on the Artemin–GFRα3 Complex

The 2-fold related potential RET binding sites are circled in dotted lines. Colored and labeled residues are conserved in GFRα receptors and surface-exposed in the GFRα3 structure. The magenta patch in ARTN are the corresponding regions found in GDNF to be important for RET activation.

RET binding surface on GFRα. The RET binding region of GFRα1 has been delimited to a region analogous to the GFRα3 "D2D3" module described here (Scott and Ibanez, 2001). Given the shared usage of RET by all GFL–GFRα complexes, the RET binding surface on GFRα may be conserved. We found 12 conserved GFRα residues that map onto an exposed face, involving both D2 and D3, on one side of GFRα3 in the complex, thereby defining a potential RET binding site (Figure 7). Most of these conserved residues are charged, which is consistent with homolog-scanning mutagenesis of RET, indicating that charged residues in the first cadherin-like domain of RET are important for formation of GDNF–GFRα1–RET complex (Kjaer and Ibanez, 2003). We propose that this face of GFRα3 forms part of the RET binding surface and includes residues from helices α2, α3, α7, α8, α9, and α10. This RET binding surface would be located adjacent to the two bottom fingers in ARTN (magenta highlighted in Figure 7), which could form part of the composite RET interaction surface. These ARTN residues do not interact with GFRα3; however, they are located within a region previously shown using GFL homolog scanning mutagenesis to be essential for RET activation (Baloh et al., 2000b). Although there are several conserved residues on the opposite face of GFRα3, it is less likely to serve as the RET binding surface due to the presence of a bulky Asparagine (309)-linked glycan prominently in the middle of the region of possible interaction (Figure 7). The two potential RET binding surfaces we proposed here are related by the intrinsic 2-fold symmetry and also angled toward one another in roughly a V-shape, such that two RET molecules, if bound along the approximate long axis of the GFRα, would be steered into closer apposition as it enters the cell membrane, resulting in reduced proximity of their intracellular kinase domains.

Experimental Procedures

Protein Preparation

Proteins used in this study were expressed using the Baculovirus system (Pharmingen) in insect cells. Briefly, insect *Spodoptera frugiperda* (Sf9) cells were used for generating high titer recombinant virus and were cultured at 28ºC using SF900 II SFM medium (Invitrogen). *Trichopulsia ni* (High-Five) cells (Invitrogen) were used to express the recombinant protein and were grown in Insect Xpress medium (Cambrex) at 28ºC. Human GFRα3 ectodomain (residues Asp32–Pro363) with C-terminal hexa-histidine and the N-terminal truncated human ARTN (Gly139–Gly237) were cloned into the pAcgp67A vector (Pharmingen). The ARTN–GFRα3 complexes were obtained by coexpression in High-Five cells and purified by Ni-NTA, FPLC Superdex 200 size exclusion, and Mono S ion-exchange columns (Pharmacia). Unbound ARTN was also expressed in High-Five cells and purified by Ni-NTA and Superdex 200 size exclusion column.

Crystallization and Data Collection

Crystals of ARTN–GFRα3 complex were grown by hanging-drop vapor diffusion at 20ºC. The well solution contained 0.1 M Imidazole (pH 8.0), 20% (v/v) ethanol, and 0.1 M $MgCl_2$. The crystals grew to a maximum size of 0.2 × 0.1 × 0.05 mm^3 over the course of 15–20 days. The crystals belong to the $P2_1$ space group and contain one full complex per asymmetric unit. Two different forms of ARTN crystals (spacegroup $P6_522$ and $P6_5$, respectively) were obtained at 20ºC with hanging-drop vapor diffusion method. One was grown with the well solution of 0.1 M Hepes (pH 7.5), 12%–16% (w/v) PEG3350, and 0.1 M $MgCl_2$, the other one with the well solution of 0.1 M Bis-Tris propane (pH 7.0) and 3 M $NaNO_3$. All data were collected at Advanced Light Source (UC Berkeley) and Stanford Synchrotron Radiation Laboratory. The data sets were collected at 100 K and processed using HKL2000 software suite (Otwinowski and Minor, 1997). More statistics of crystal and data collection are in Table 1.

Structure Determination and Refinement

The structure of unbound ARTN was first determined by single isomorphous replacement with anomalous scattering (SIRAS) method with a mercury derivative in $P6_5$ form, which has three dimers in the asymmetric unit. The derivative was prepared by soaking a single crystal in the mother liquor containing 100 mM Thimerosal for 1 hr. The heavy atom binding sites were determined with SHELXD (Schneider and Sheldrick, 2002). The initial phases were calculated in SHARP (de la Fortrelle and Bricogne, 1997) and improved with SOLOMON (Abrahams and Leslie, 1996). The ARTN model from $P6_5$ form was used to determine its structure in $P6_522$ form (one monomer per asymmetric unit) with PHASER (Read, 2001). The structure of the ARTN–GFRα3 complex was determined by the molecular replacement method with our ARTN and GFRα1 D3 domain structures (PDB ID: 1Q8D) as the search models. Program PHASER (Read, 2001) was used to locate the positions of one ARTN dimer and two GFRα3 D3 domains in the complex. After density improvement with ARP/wARP (Perrakis et al., 1999), the residues in the D2 domain were built into the map by using COOT (Emsley and Cowtan, 2004). All structures were refined with CNS (Brunger et al., 1998) and REFMAC (CCP4 package) (Murshudov et al., 1997). Structure determination and refinement statistics are listed in Table 1.

Isothermal Titration Calorimetry (ITC) and Multiangle Light Scattering (MALS)

Calorimetry titrations were carried out on the VP-ITC calorimeter (MicroCal) at 20ºC, with 15 μM GFRα3 titrated against 2.5 μM ARTN dimer. Both GFRα3 and ARTN were prepared in a buffer containing 0.01 M Hepes (pH 7.2) and 0.5 M NaCl. The data were processed with the MicroCal Origin 7.0 software. A DAWN EOS (Wyatt Technology) equipped with a K5 flow cell and a 30 mW linearly polarized GaAs laser of wavelength 690 nm was used in MALS experiment. Data analysis was carried out real time using ASTRA (Wyatt

Technologies) and molecular weight was calculated using the Debye fit method.

Receptor Activation Assays

They were performed as described previously (Baloh et al., 2000b). Briefly, 3T3 fibroblasts stably expressing human RET were plated at 85,000 cells/well in 12-well plates and transfected using Superfect (Qiagen) with the reporter plasmids (250 ng/well Gal4-Luc, 50 ng/well Gal4-Elk), CMV-lacZ (50 ng/well) for transfection normalization, a CMV-GFRα (500 ng/well) expression plasmid, and 650 ng/well pBluescript as a carrier for a total of 1.5 μg of DNA/well. Cells were switched to 0.5% serum-containing medium the morning after transfection, stimulated for 6 hr with 50 ng ml^{-1} of recombinant artemin or neurturin, and harvested 36 hr after transfection. The average luciferase activity of triplicate samples was normalized to β-galactosidase activity of the cotransfected lacZ reporter to control for transfection efficiency.

Supplemental Data

Supplemental data including a supplemental figure and table are available at http://www.structure.org/cgi/content/full/14/6/1083/DC1/.

Acknowledgments

We thank N. Goriatcheva and D. Waghray for expert technical assistance, S. Juo and S. Laporte for assistance with data collection, F. Bazan for critical reading of the manuscript, S. Jain for the image of RET-GFP neurons, C. Ibanez for the gift of GFRα3 DNA, A. Bankovich for help in biophysical experiments, and M. Rickert for help in making figures. This work was supported by NIH grants AG13730 and NS39358 (J.M.), The Keck Foundation (KCG), NIH RO1 HL077325 (KCG), The Christopher Reeve Paralysis Foundation (KCG), and The Howard Hughes Medical Institute (KCG).

Received: May 11, 2006
Revised: May 17, 2006
Accepted: May 17, 2006
Published: June 13, 2006

References

Abrahams, J.P., and Leslie, A.G. (1996). Methods used in the structure determination of bovine mitochondrial F1 ATPase. Acta Crystallogr. D Biol. Crystallogr. *52*, 30–42.

Airaksinen, M.S., and Saarma, M. (2002). The GDNF family: signalling, biological functions and therapeutic value. Nat. Rev. Neurosci. *3*, 383–394.

Airaksinen, M.S., Titievsky, A., and Saarma, M. (1999). GDNF family neurotrophic factor signaling: four masters, one servant? Mol. Cell. Neurosci. *13*, 313–325.

Allendorph, G.P., Vale, W.W., and Choe, S. (2006). Structure of the ternary signaling complex of a TGF-beta superfamily member. Proc. Natl. Acad. Sci. USA *103*, 7643–7648.

Baloh, R.H., Tansey, M.G., Lampe, P.A., Fahrner, T.J., Enomoto, H., Simburger, K.S., Leitner, M.L., Araki, T., Johnson, E.M., Jr., and Milbrandt, J. (1998). Artemin, a novel member of the GDNF ligand family, supports peripheral and central neurons and signals through the GFRalpha3-RET receptor complex. Neuron *21*, 1291–1302.

Baloh, R.H., Enomoto, H., Johnson, E.M., Jr., and Milbrandt, J. (2000a). The GDNF family ligands and receptors - implications for neural development. Curr. Opin. Neurobiol. *10*, 103–110.

Baloh, R.H., Tansey, M.G., Johnson, E.M., Jr., and Milbrandt, J. (2000b). Functional mapping of receptor specificity domains of glial cell line-derived neurotrophic factor (GDNF) family ligands and production of GFRalpha1 RET-specific agonists. J. Biol. Chem. *275*, 3412–3420.

Brunger, A.T., Adams, P.D., Clore, G.M., DeLano, W.L., Gros, P., Grosse-Kunstleve, R.W., Jiang, J.S., Kuszewski, J., Nilges, M., Pannu, N.S., et al. (1998). Crystallography & NMR system: A new software suite for macromolecular structure determination. Acta Crystallogr. D Biol. Crystallogr. *54*, 905–921.

Buj-Bello, A., Adu, J., Pinon, L.G., Horton, A., Thompson, J., Rosenthal, A., Chinchetru, M., Buchman, V.L., and Davies, A.M. (1997). Neurturin responsiveness requires a GPI-linked receptor and the Ret receptor tyrosine kinase. Nature *387*, 721–724.

Carneiro, F.A., Bianconi, M.L., Weissmuller, G., Stauffer, F., and Da Poian, A.T. (2002). Membrane recognition by vesicular stomatitis virus involves enthalpy-driven protein-lipid interactions. J. Virol. *76*, 3756–3764.

de la Fortrelle, E., and Bricogne, G. (1997). Maximum-likelihood heavy atom parameter refinement for multiple isomorphous replacement and multiwavelength anomalous diffraction methods. Methods Enzymol. *276*, 472–494.

DeLano, W.L. (2002). The PyMOL Molecular Graphics System (San Carlos, CA: DeLano Scientific).

Durbec, P., Marcos-Gutierrez, C.V., Kilkenny, C., Grigoriou, M., Wartiowaara, K., Suvanto, P., Smith, D., Ponder, B., Costantini, F., Saarma, M., et al. (1996). GDNF signalling through the Ret receptor tyrosine kinase. Nature *381*, 789–793.

Eigenbrot, C., and Gerber, N. (1997). X-ray structure of glial cell-derived neurotrophic factor at 1.9 A resolution and implications for receptor binding. Nat. Struct. Biol. *4*, 435–438.

Eketjall, S., Fainzilber, M., Murray-Rust, J., and Ibanez, C.F. (1999). Distinct structural elements in GDNF mediate binding to GFRalpha1 and activation of the GFRalpha1-c-Ret receptor complex. EMBO J. *18*, 5901–5910.

Emsley, P., and Cowtan, K. (2004). Coot: model-building tools for molecular graphics. Acta Crystallogr. D Biol. Crystallogr. *60*, 2126–2132.

Enokido, Y., de Sauvage, F., Hongo, J.A., Ninkina, N., Rosenthal, A., Buchman, V.L., and Davies, A.M. (1998). GFR alpha-4 and the tyrosine kinase Ret form a functional receptor complex for persephin. Curr. Biol. *8*, 1019–1022.

Gardell, L.R., Wang, R., Ehrenfels, C., Ossipov, M.H., Rossomando, A.J., Miller, S., Buckley, C., Cai, A.K., Tse, A., Foley, S.F., et al. (2003). Multiple actions of systemic artemin in experimental neuropathy. Nat. Med. *9*, 1383–1389.

Gill, S.S., Patel, N.K., Hotton, G.R., O'Sullivan, K., McCarter, R., Bunnage, M., Brooks, D.J., Svendsen, C.N., and Heywood, P. (2003). Direct brain infusion of glial cell line-derived neurotrophic factor in Parkinson disease. Nat. Med. *9*, 589–595.

Greenwald, J., Groppe, J., Gray, P., Wiater, E., Kwiatkowski, W., Vale, W., and Choe, S. (2003). The BMP7/ActRII extracellular domain complex provides new insights into the cooperative nature of receptor assembly. Mol. Cell *11*, 605–617.

Greenwald, J., Vega, M.E., Allendorph, G.P., Fischer, W.H., Vale, W., and Choe, S. (2004). A flexible activin explains the membrane-dependent cooperative assembly of TGF-beta family receptors. Mol. Cell *15*, 485–489.

Grondin, R., and Gash, D.M. (1998). Glial cell line-derived neurotrophic factor (GDNF): a drug candidate for the treatment of Parkinson's disease. J. Neurol. *245*, 35–42.

Hart, P.J., Deep, S., Taylor, A.B., Shu, Z., Hinck, C.S., and Hinck, A.P. (2002). Crystal structure of the human TbetaR2 ectodomain–TGF-beta3 complex. Nat. Struct. Biol. *9*, 203–208.

He, X., Chow, D., Martick, M.M., and Garcia, K.C. (2001). Allosteric activation of a spring-loaded natriuretic peptide receptor dimer by hormone. Science *293*, 1657–1662.

Jing, S., Wen, D., Yu, Y., Holst, P.L., Luo, Y., Fang, M., Tamir, R., Antonio, L., Hu, Z., Cupples, R., et al. (1996). GDNF-induced activation of the ret protein tyrosine kinase is mediated by GDNFR-alpha, a novel receptor for GDNF. Cell *85*, 1113–1124.

Kirsch, T., Sebald, W., and Dreyer, M.K. (2000). Crystal structure of the BMP-2-BRIA ectodomain complex. Nat. Struct. Biol. *7*, 492–496.

Kjaer, S., and Ibanez, C.F. (2003). Identification of a surface for binding to the GDNF-GFR alpha 1 complex in the first cadherin-like domain of RET. J. Biol. Chem. *278*, 47898–47904.

Kotzbauer, P.T., Lampe, P.A., Heuckeroth, R.O., Golden, J.P., Creedon, D.J., Johnson, E.M., Jr., and Milbrandt, J. (1996). Neurturin, a relative of glial-cell-line-derived neurotrophic factor. Nature *384*, 467–470.

Leppanen, V.M., Bespalov, M.M., Runeberg-Roos, P., Puurand, U., Merits, A., Saarma, M., and Goldman, A. (2004). The structure of GFRalpha1 domain 3 reveals new insights into GDNF binding and RET activation. EMBO J. *23*, 1452–1462.

Lin, L.F., Doherty, D.H., Lile, J.D., Bektesh, S., and Collins, F. (1993). GDNF: a glial cell line-derived neurotrophic factor for midbrain dopaminergic neurons. Science *260*, 1130–1132.

Massague, J., and Chen, Y.G. (2000). Controlling TGF-beta signaling. Genes Dev. *14*, 627–644.

Milbrandt, J., de Sauvage, F.J., Fahrner, T.J., Baloh, R.H., Leitner, M.L., Tansey, M.G., Lampe, P.A., Heuckeroth, R.O., Kotzbauer, P.T., Simburger, K.S., et al. (1998). Persephin, a novel neurotrophic factor related to GDNF and neurturin. Neuron *20*, 245–253.

Murshudov, G.N., Vagin, A.A., and Dodson, E.J. (1997). Refinement of macromolecular structures by the maximum-likelihood method. Acta Crystallogr. D Biol. Crystallogr. *53*, 240–255.

Otwinowski, Z., and Minor, W. (1997). Processing of X-ray diffraction data collected in oscillation mode. Methods Enzymol. *276*, 307–326.

Perrakis, A., Morris, R., and Lamzin, V.S. (1999). Automated protein model building combined with iterative structure refinement. Nat. Struct. Biol. *6*, 458–463.

Read, R.J. (2001). Pushing the boundaries of molecular replacement with maximum likelihood. Acta Crystallogr. D Biol. Crystallogr. *57*, 1373–1382.

Saarma, M. (2000). GDNF - a stranger in the TGF-beta superfamily? Eur. J. Biochem. *267*, 6968–6971.

Schneider, T.R., and Sheldrick, G.M. (2002). Substructure solution with SHELXD. Acta Crystallogr. D Biol. Crystallogr. *58*, 1772–1779.

Scott, R.P., and Ibanez, C.F. (2001). Determinants of ligand binding specificity in the glial cell line-derived neurotrophic factor family receptor alpha S. J. Biol. Chem. *276*, 1450–1458.

Slevin, J.T., Gerhardt, G.A., Smith, C.D., Gash, D.M., Kryscio, R., and Young, B. (2005). Improvement of bilateral motor functions in patients with Parkinson disease through the unilateral intraputaminal infusion of glial cell line-derived neurotrophic factor. J. Neurosurg. *102*, 216–222.

Sun, P.D., and Davies, D.R. (1995). The cystine-knot growth-factor superfamily. Annu. Rev. Biophys. Biomol. Struct. *24*, 269–291.

Thompson, T.B., Woodruff, T.K., and Jardetzky, T.S. (2003). Structures of an ActRIIB:activin A complex reveal a novel binding mode for TGF-beta ligand:receptor interactions. EMBO J. *22*, 1555–1566.

Treanor, J.J., Goodman, L., de Sauvage, F., Stone, D.M., Poulsen, K.T., Beck, C.D., Gray, C., Armanini, M.P., Pollock, R.A., Hefti, F., et al. (1996). Characterization of a multicomponent receptor for GDNF. Nature *382*, 80–83.

Trupp, M., Arenas, E., Fainzilber, M., Nilsson, A.S., Sieber, B.A., Grigoriou, M., Kilkenny, C., Salazar-Grueso, E., Pachnis, V., and Arumae, U. (1996). Functional receptor for GDNF encoded by the c-ret proto-oncogene. Nature *381*, 785–789.

Trupp, M., Raynoschek, C., Belluardo, N., and Ibanez, C.F. (1998). Multiple GPI-anchored receptors control GDNF-dependent and independent activation of the c-Ret receptor tyrosine kinase. Mol. Cell. Neurosci. *11*, 47–63.

Worby, C.A., Vega, Q.C., Zhao, Y., Chao, H.H., Seasholtz, A.F., and Dixon, J.E. (1996). Glial cell line-derived neurotrophic factor signals through the RET receptor and activates mitogen-activated protein kinase. J. Biol. Chem. *271*, 23619–23622.

York, R.D., Yao, H., Dillon, T., Ellig, C.L., Eckert, S.P., McCleskey, E.W., and Stork, P.J. (1998). Rap1 mediates sustained MAP kinase activation induced by nerve growth factor. Nature *392*, 622–626.

Accession Numbers

The coordinates have been deposited in the RCSB Protein Data Bank with the accession codes: 2GH0 (ARTN−GFRα3 complex), 2GYR (ARTN) and 2GYZ (ARTN).

Supplementary Data

Structure of Artemin Complexed with Its Receptor GFRα3: Convergent Recognition of Glial Cell Line-Derived Neurotrophic Factors

Xinquan Wang,[1] Robert H. Baloh,[2] Jeffrey Milbrandt,[3] and K. Christopher Garcia[1,*]

[1]Howard Hughes Medical Institute

Stanford University School of Medicine

Departments of Microbiology and Immunology, and Structural Biology

Stanford, California, 94305-5124

[2]Department of Neurobiology

Washington University School of Medicine

St. Louis, Missouri 63110

[3]HOPE Center for Neurological Disorders

Departments of Pathology and Neurology

Washington University School of Medicine

St. Louis, Missouri 63110

*Correspondence: kcgarcia@stanford.edu

Ph: 650-498-7332, Fax: 650-725-6757

Table S1. Contact residues in the binding interface (d < 4.5 Å)

ARTN contact residue	GFRα3 contact residue
L129	T170, L171
D142	L163
E143	L163, M167, R179, R230
L144	M167, T170
V145	T170, K180,
R146	T170, L171, N172, D173, D176, K180
R148	R177, D176
A195	E184, K180
V196	K180
S197	R179, K180, G183, E184, S187
M199	R179, R230, N233, T234
N202	E229, N233,
S203	E229, R230, N233
W205	R179, Y182, G183, S187, G188, N233, T234, A236
R206	S187
T207	G183, E184, S187

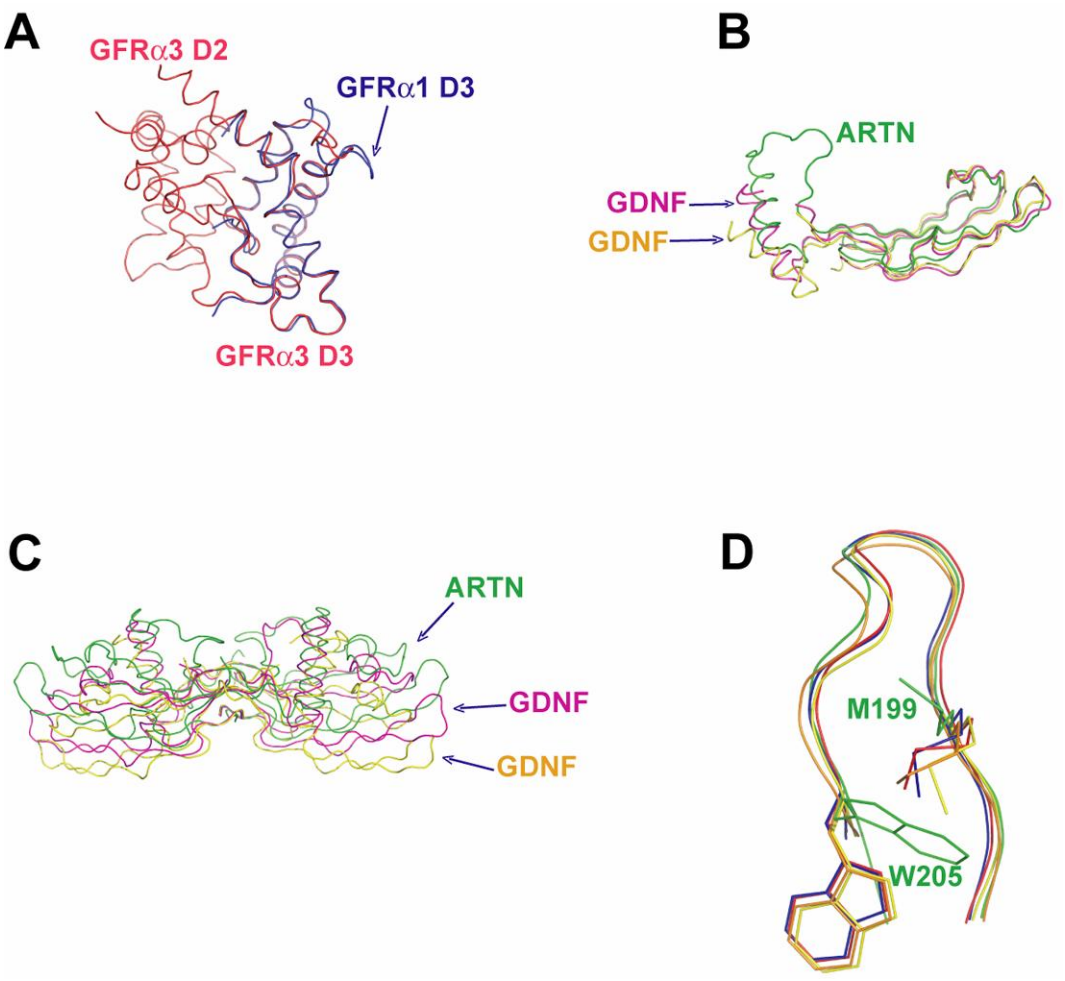

Figure S1. Structural Comparison

(A) Superposition of GFRα3 and GFRα1 D3 domains.

(B) Superposition of ARTN (green) and two independent GDNF (yellow and purple) monomers shows the difference of the angle between heel and finger regions in the momoer.

(C) Superposition of ARTN (green) and two independent GDNF (yellow and purple) dimers show the different inter-dimer angles.

(D) The side chain conformational changes of Met199 and Trp205 in ARTN upon complex formation. ARTN in complex is shown in green, while others are the structures of unbound ARTN in $P6_522$ and $P6_5$ crystal forms.